Growth of CdS Nanorods in Nonionic Amphiphilic Triblock Copolymer Systems

Chung-Sung Yang,† David D. Awschalom,‡ and Galen D. Stucky*,†

Department of Chemistry and Biochemistry and Department of Physics, University of California, Santa Barbara, California 93106

Received September 3, 2001. Revised Manuscript Received November 2, 2001

Size-tunable CdS nanorods have been synthesized via the reaction at low temperature (25−65 °C) of air-insensitive inorganic precursors cadmium acetate and sodium sulfide in an aqueous phase with surfactant. Nonionic pluronic amphiphilic triblock copolymers, $(EO)_x(PO)_y(EO)_x$, were employed as structure-directing agents. The effects of the (EO)/(PO) ratio, surfactant size, and mole ratio between surfactant and precursors in controlling the diameter and the morphology of the final product were investigated. Transmission electron microscopy (TEM) images show that the diameter of the CdS nanorods synthesized by this method can be controlled by varying the surfactant species, the mole ratio between the inorganic precursors and triblock copolymer, and the reaction temperature. However, if the reaction is refluxed in organic solvent (ethylene glycol and glyme) without surfactant, the morphology of the product will change to microrods with flat ends, dumbbell-shaped microrods, and cotton-ball-like microparticles. The hydrophilic poly(ethylene oxide) fraction, $(EO)_x$, of the triblock copolymers plays a decisive role in controlling the morphology of the final product, and the hydrophobic poly(isopropylene oxide) fraction, $(PO)_y$, affects the diameter of the nanocrystallites. The typical size of CdS nanorods synthesized using $(EO)_{20}(PO)_{70}(EO)_{20}$ is about 5.0−7.0 nm in diameter and 30−90 nm in length. The X-ray powder diffraction pattern is consistent with the hexagonal wurtzite crystal structure. This low-temperature aqueous synthesis route can be considered as an environmentally friendly and inexpensive method of producing nearly monodisperse CdS particles and arrays (σ < 10%).

Introduction

One-dimensional nanorods have been the focus of intensive interest recently because of their vital role as interconnect components in future mesoscopic electronic and optical devices.[1] Control of the size, especially the diameter, is a key factor in the success of nanorod synthesis. To date, various methods have been reported for achieving this purpose, with much of the effort focused on the synthesis of III−V semiconductors. Synthetic methods employing solution−liquid−solid (SLS) growth of III−V semiconductors, such as InP and InAs, at temperatures below 203 °C produce a broad distribution of diameters (10−150 nm).[2] Carbon-nanotube-confined reactions using vapor deposition give good-quality GaN nanorods with diameter reportedly equal to those of the carbon nanotubes (4−50 nm).[3] Electrochemical fabrication using porous aluminum oxide as the template produces extremely large length/diameter (L/D) ratios (∼120, with length = 1000−2400 nm and diameter = 9−20 nm) mainly because of the size of the pore and the thickness of the template.[4] The polymer cluster growth method does not control the growing direction well and leads to a wool-ball-like morphology.[5] Nonaqueous synthesis displays a wide size distribution in both length and diameter, with lengths in the range 300−2500 nm and diameters in the range 25−75 nm.[6] The laser ablation technique has recently been used with great success in the synthesis of Si, Ge, and InP nanowires[7,8] but has not been demonstrated for the synthesis of II−VI binary semiconductor nanorods. The most promising of the current technologies to offer a narrow distribution of diameters in II−VI binary semiconductor nanorods synthesis is the use of an air-sensitive starting reagent, dimethyl cadmium, and a two-surfactant system, trioctyl phosphate oxide (TOPO) and hexylphosphonic acid (HPA), to control the morphology and diameter of the nanorods that are formed.[9−11]

We present a simple and reliable low-temperature aqueous synthesis route using air-insensitive starting

* Author to whom correspondence should be addressed.
† Department of Chemistry and Biochemistry.
‡ Department of Physics.

(1) Alivisatos, A. P. *Science* **1996**, *271*, 933−937.
(2) Trentler, T. J.; Hickman, K. M.; Goel, S. C.; Viano, A. M.; Gibbons, P. C.; Buhro, W. E. *Science* **1995**, *270*, 1791−1794.
(3) Han, W.; Fan, S.; Li, Q.; Hu, Y. *Science* **1997**, *277*, 1287−1289.
(4) Routkevitch, D.; Bigiomi, T.; Moskovits, M.; Xu, J. M. *J. Phys. Chem.* **1996**, *100*, 14037−14047.
(5) Yan, P.; Xie, Y.; Qian, Y.; Liu, X. *Chem. Commun.* **1999**, 1293−1294.
(6) Li, Y.-D.; Liao, H.-W.; Ding, Y.; Qian, Y.-T.; Yang, L.; Zhou, G.-E. *Chem. Mater.* **1998**, *10*, 2301−2303.
(7) Morales, A. M.; Lieber, C. M. *Science* **1998**, *279*, 208−211.
(8) Duan, X. F.; Huang, Y.; Cui, Y.; Wang, J. F.; Lieber, C. M. *Nature* **2001**, *409*, 66−69.
(9) Peng, X.; Manna, L.; Yang, W.; Wickham, J.; Scher, E.; Kadavanich, A.; Alivisatos, A. P. *Nature* **2000**, *404*, 59−61.
(10) Yang, C.-S.; Awschalom, D., D.; Stucky, G. D. *Chem. Mater.* **2001**, *13*, 594−598.
(11) Manna, L.; Scher, E.; Alivisatos, A. P. *J. Am. Chem. Soc.* **2000**, *122*, 12700−12706.

10.1021/cm011227b CCC: $22.00
Published on Web 01/29/2002

reagents and triblock copolymers to produce narrow-size-distribution CdS nanorods (NRs) with dominant diameters varying in a nearly monodisperse region (σ < 10%). The Pluronic triblock copolymers series poly(ethylene glycol)-*block*-poly(propylene glycol)-*block*-poly(ethylene glycol), $H(-OCH_2CH_2)_x[-OCH(CH_3)-CH_2]_y(-OCH_2CH_2)_y-OH$ or $(EO)_x(PO)_y(EO)_x$, which has demonstrated excellent properties for the synthesis of mesoporous materials,[12−14] is used as surfactant templates and initiates the nucleation of the nanoparticles at room temperature. The crystal quality can be improved by annealing the sample at 65 °C for 1 h. The X-ray diffraction patterns of the annealed samples show no evidence of a mixed phase after annealing.

Experimental Section

(I) Synthesis of CdS Rods in an Organic Solvent without Surfactant. In this route, CdS rods were synthesized by refluxing at 86−198 °C without surfactant using ethylene glycol (EG), ethylene glycol dimethyl ether (glyme), or a mixture of the two chemicals as the solvent. After cadmium acetate (2×10^{-3} M) and sodium sulfide (2×10^{-3} M) had been refluxed in 50 mL of solvent for 4 h, the product was allowed to cool slowly to room temperature, and the yellow precipitate was collected by overnight precipitation. The product was suspended in methanol and dried as a powder for further X-ray powder diffraction study.

(II) Synthesis of CdS Nanorods in an Aqueous Phase with Surfactant. The Pluronic amphiphilic triblock copolymers L121 $[(EO)_5(PO)_{70}(EO)_5]$, L64 $[(EO)_{13}(PO)_{70}(EO)_{13}]$, P123 $[(EO)_{20}(PO)_{70}(EO)_{20}]$, P65 $[(EO)_{20}(PO)_{30}(EO)_{20}]$, F127 $[(EO)_{106}(PO)_{70}(EO)_{106}]$, and F68 $[(EO)_{80}(PO)_{30}(EO)_{80}]$, all obtained from BASF, were each dissolved completely in deionized water at a mole ratio of triblock copolymer to H_2O of 1:10 000, and the resulting solutions were saved as stock solvents. CdS nanocrystals were synthesized by the reaction of cadmium acetate and sodium sulfide purchased from Aldrich in the stock solvents. The triblock copolymer: $Cd^{2+}/S^{2-}/H_2O$ mole ratio was set at 1:10:10:10 000. The reactions were performed in a Schlenk line under N_2 atmosphere, and the temperature was increased gradually from room temperature to 40 or 65 °C. The reactions were allowed to proceed for 16 h with moderate stirring (180−240 rpm). The resulting solution was centrifuged for 5 min, and a yellow to orange-red precipitate was obtained, depending on the surfactant template species. After removal of the supernatant, the remaining product was twice washed with 25 mL of a 50:50 ether/ethanol mixture and then once with 15 mL of methanol to remove the surfactant residue. The final precipitate can be dried as a powder or resuspended in methanol or ethanol.

X-ray powder diffraction data were obtained on a Scintag X_2 instrument. Samples were deposited onto glass slips, and data were measured at room temperature using Cu $K\alpha_1$ radiation. Transmission electron microscopy (TEM) images and energy dispersion spectra (EDS) were collected on a JEOL 2000FX instrument with a 200-keV accelerating voltage, and high-resolution TEM images were obtained with a JEOL 2010HR instrument. Samples were prepared by evaporation of colloids onto a 200-mesh Cu grid at room temperature. Scanning electron microscopy (SEM) images were obtained with a JEOL JSM 6300F instrument using a 3-keV scanning voltage. Samples were deposited onto glass substrates and coated with Au/Pd by ion sputtering at room temperature. Optical absorption spectra of methanol colloids in a quartz cell were obtained with a Shimadzu UV 1601 spectrophotometer. Photoluminescence spectra were obtained using a SPEX FluoroMax spectrophotometer with an excitation wavelength at 360 nm. All spectra were collected at room temperature.

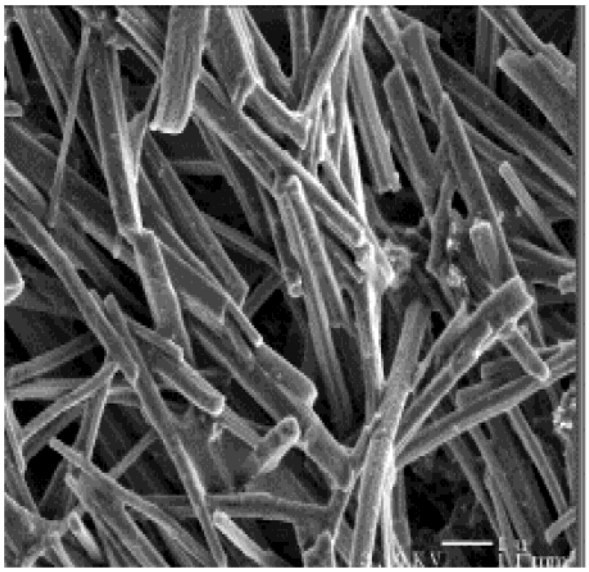

Figure 1. Scanning electron microscopy (SEM) micrograph showing that the morphology of rod-1 is a uniformly flat-ended rod with an average length of >4 μm and diameters between 0.2 and 0.4 μm.

Results

In this paper, the parameters chosen to study the influence on the crystal-growth mechanism of CdS nanorods in Pluronic triblock copolymer system included the solvent, the surfactant species, the (EO)/(PO) ratio of the surfactant, the reaction temperature, and the mole ratios between the surfactant and the inorganic precursors.

(I) Synthesis of CdS Rods in an Organic Solvent without Surfactant. *(a) 100% Ethylene Glycol (EG).* EG was chosen as a solvent for synthesis of the nanorods because each EG molecule has two active OH groups to chelate with Cd cations and has a relatively weak intermolecular coordinating force, which allows the products to grow in a less confined environment.[15] Scanning electron microscopy (SEM) (Figure 1) clearly shows that the general morphology of the product is that of a uniform flat-ended rod with an average length of >4 μm and a diameter of 0.2−0.6 μm (rod-1). The flat-ended morphology suggests that the shape evolution mechanism[16] is not the case in this synthesis. The morphology of rod-1 is generally consistent with kinetically controlled crystal growth.[17] The surface of the product is smooth and shiny and attached with a small number of nanoparticles. Rod-1 is stable in methanol or ethanol and can survive 3-keV electron beams without deterioration. The X-ray powder diffraction pattern shows that the structure of rod-1 is a mixed phase of hexagonal wurtzite and cubic zinc blende, which is generally consistent with the literature.[18−20]

(12) Zhao, D.; Feng, J.; Huo, Q.; Melosh, N.; Fredrickson, G. H.; Chmelka, B. F.; Stucky, G. D. *Science* **1998**, *279*, 548−552.
(13) Kim, J. M.; Stucky, G. D. *Chem. Commun.* **2000**, 1159−1160.
(14) Feng, P.; Bu, X.; Stucky, G. D.; Pine, D. J. *J. Am. Chem. Soc.* **2000**, *122*, 994−995.
(15) Li, Y.; Liao, H.; Ding, Y.; Fan, Y.; Zhang, Y.; Qian, Y. *Inorg. Chem.* **1999**, *38*, 1382−1387.
(16) Peng, Z. A.; Peng, X. *J. Am. Chem. Soc.* **2001**, *123*, 1389−1395.
(17) Mullin, J. W. *Crystallization*, 3rd ed.; Butterworth-Heinemann: Woburn, MA, 1997.
(18) Manna, L.; Scher, E. C.; Alivisatos, A. P. *J. Am. Chem. Soc.* **2000**, *122*, 12700−12706.

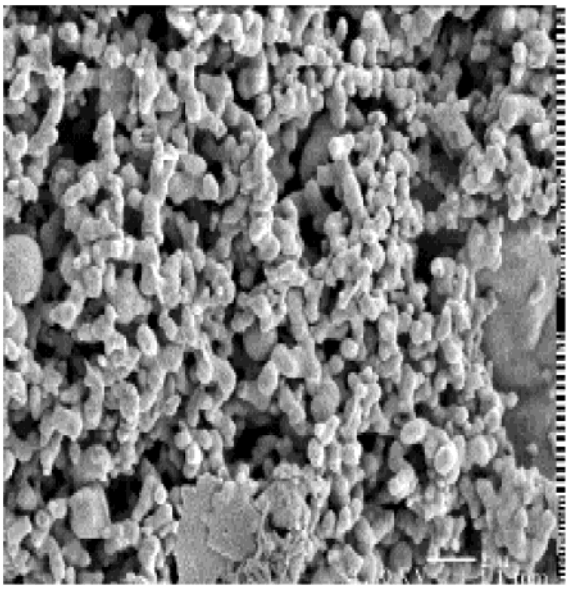

Figure 2. SEM image containing a large number of rod-2, dumbbell-shaped rods with rough surfaces, synthesized from the reaction in 80% EG + 20% glyme. The average length of rod-2 is about 2 μm and the diameter is about 0.3 μm, which are both smaller than the corresponding values for rod-1.

(b) 80% EG + 20% Ethylene Glycol Dimethyl Ether (Glyme). Ten milliliters of glyme was mixed with 40 mL of EG to study the effect of cosolvent. Glyme series solvents, which have shown their excellent capabilities in the synthesis of Si nanoparticles,[21,22] have longer alkyl chains than EG and are expected to have stronger coordinating forces that confine the product to grow in a tighter space. The boiling point of the mixed solvent decreases to 150−160 °C. The same synthesis route was performed, and the yellow product was collected after a 16-h slow precipitation. Figure 2 shows that the predominant morphology of the product (rod-2) is dumbbell-shaped with rough surface. The average length is about 2 μm, with a typical diameter of 0.3 μm. The sizes of rod-2 are generally smaller than those of rod-1 in both diameter and length. This is probably because the formation constant of glyme−Cd is smaller than that of EG−Cd. The CdS growth in glyme−Cd complex is less directed by the solvent−inorganic interface interaction than it is for EG−Cd.[16] The product has a narrower diameter distribution than rod-1.

(c) 50% EG + 50% Glyme and 100% Glyme. When the volume ratio of glyme is increased to 50%, the morphology of the product remains dumbbell-shaped but the yield is noticeably lower than that of rod-2. The construction of spherical aggregates increases dramatically, and the aspect ratio of the dumbbell-shaped rods decreases, with an average length of ~1 μm and diameters between 0.3 and 0.4 μm. In the 100% glyme synthesis route, there is no evidence of any flat-ended or dumbbell-shaped rods. Instead, a large number of spherical particles (diameters generally between 0.55 and 0.75 μm), like soft cotton balls, are found in the final product. The results are consistent with the weak Cd−glyme interface interactions that lead to nondirectional growth.

(II) Synthesis of CdS Nanorods in an Aqueous Phase with Pluronic $(EO)_x(PO)_y(EO)_x$ Triblock Copolymer as Surfactant Templates. The series of Pluronic triblock copolymers $(EO)_x(PO)_y(EO)_x$ was chosen as surfactant templates for the low-temperature (25−65 °C) surfactant-dependent synthesis because they can initiate nucleation of the nanoparticles at room temperature and because they offer an amphiphilic environment, which EG and glyme cannot offer, with hydrophilic/hydrophobic domain fractions in which the nanoparticles can grow. In a water-rich $(EO)_x(PO)_y(EO)_x$/water binary system, the $(EO)_x(PO)_y(EO)_x$ molecules are dissolved in water as individual unimers at room temperature. The mole ratio between surfactant and water in our experiments was set at 1:10 000. The reaction time and temperature were kept constant or varied in a way that depends on the parameter-control requirements for different surfactant-involved reactions. The seeds of CdS nanoparticles formed immediately upon addition of the inorganic starting reagents to the stock solvents. The color of the product varied with the surfactant used, including yellow-green (L121), yellow (L64), orange (P123, F68, P65), and tangerine (F127), which might be because of the different sizes of the products formed therein. Surprisingly, when suspended in methanol or ethanol, the products were stable for more than six months without any change in color.

(a) Effect of the $(EO)_x$ Fraction on the Morphology and Diameter of the CdS Nanocrystals. P123, F127, L64, and L121 were chosen to study the effect of the $(EO)_{20}$ fraction on the morphology and diameter of the CdS nanocrystals. The four chosen surfactants have the same $(PO)_y$ fraction length, namely, $y = 70$.

(1) P123 [$(EO)_{20}(PO)_{70}(EO)_{20}$], $f = 0.57$ [$f = 2x/y$, i.e., $2(EO)_x/(PO)_y$]. The morphology of the product using P123 as the surfactant template contains nanorods of uniform diameter (P123 NR-1), shown in Figure 3a, which have a fiberlike appearance with increasing length. The morphology is similar to the rod-1 structure shown in Figure 1a except that the length and diameter of P123 NR-1 are much smaller. The gray amorphous material shown in Figure 3a is the residue of surfactant P123 used in the reactions. The residue can be removed by repeated washing in hot ethanol, but the possibility of losing the uniform morphology of the nanorods increases as a result. The energy dispersion spectrum (EDS), Figure 3b, displays cadmium $L\alpha_1$ (3.13 keV), $L\alpha_2$ (3.31 keV), sulfur $K\alpha_1$ (2.30 keV), and sodium $K\alpha$ (0.94 keV) peaks. The sodium peak suggests that the nanorods might be coordinated with the sodium/surfactant template. The growth mechanisms of P123 NR-1 and rod-1 are obviously different because of the triblock copolymer hydrophilic/hydrophobic character.[23] The length of P123 NR-1 varies from 30 to 90 nm, with a few shorter products (15−30 nm). The percentage distributions in these regions are roughly similar, but

(19) Yeh, C.-Y.; Lu, Z. W.; Froyen, S.; Zunger, A. *Phys. Rev. B* **1992**, *46*, 10086−10097.
(20) Joint Committee on Powder Diffraction Standards (JCPDS) cards 41-1049, 42-1411, 10-454, and 21-829.
(21) Yang, C.-S.; Bley, R. A.; Kauzlarich, S. M.; Lee, H. W. H.; Delgado, G. R. *J. Am. Chem. Soc.* **1999**, *121*, 5191−5195.
(22) Yang, C.-S.; Kauzlarich, S. M.; Wang, Y. C.; Lee, H. W. H. *J. Cluster Sci.* **2000**, *11*, 423−431.
(23) Olshavsky, M. A.; Allcock, H. R. *Chem. Mater.* **1997**, *9*, 1367−1376.

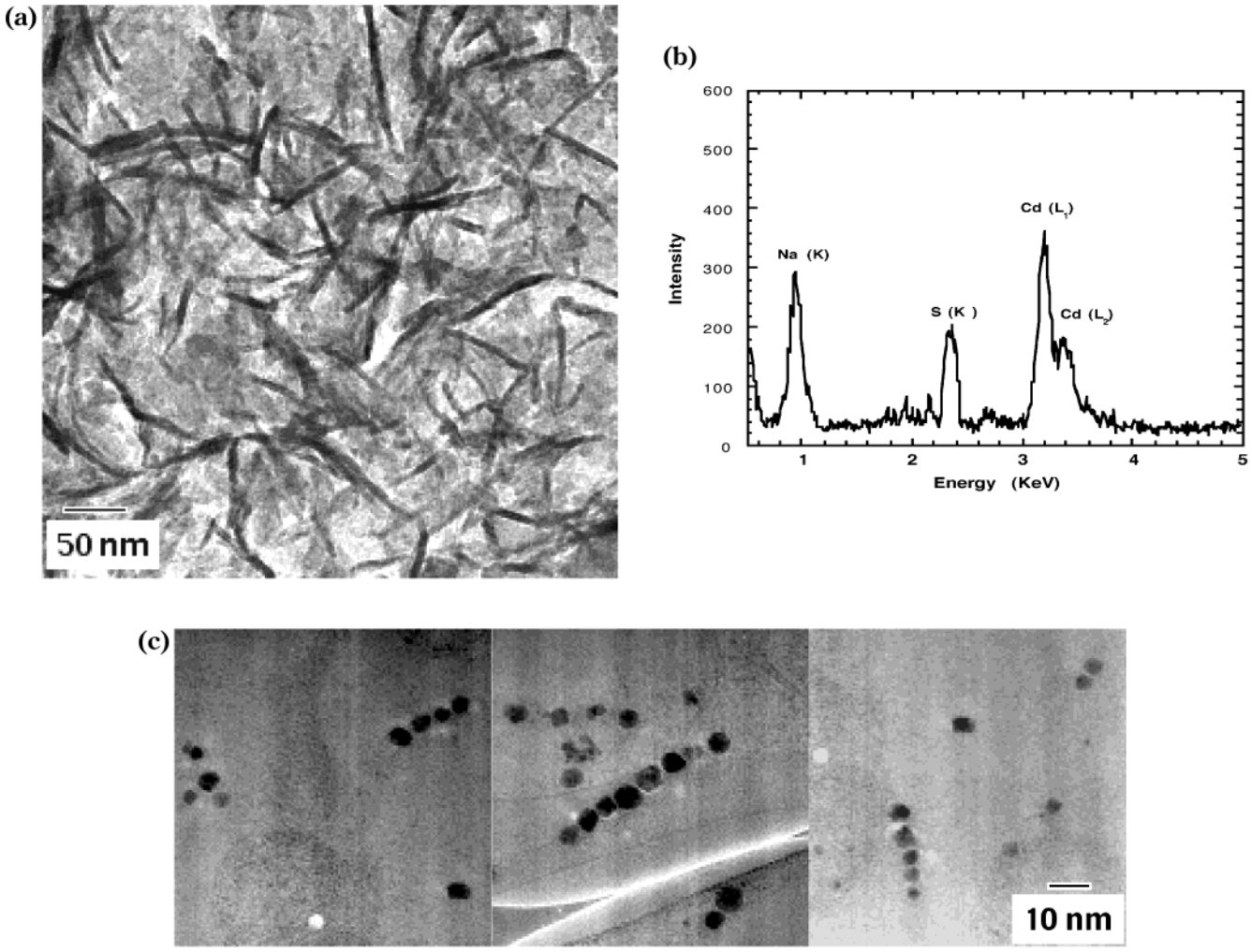

Figure 3. (a) TEM micrograph showing a large number of P123 NR-1 nanorods. The diameters vary from 5 to 7.0 nm and the length varies from 30 to 90 nm. (b) Energy dispersion spectrum (EDS) displaying cadmium $L\alpha_1$ (3.13 keV), $L\alpha_2$ (3.31 keV), sulfur $K\alpha_1$(2.30 keV), and sodium $K\alpha$ (0.94 keV) peaks. These data suggest that the P123 NR-1 nanorods contain Cd and S and that the nanorods are coordinated with the sodium/surfactant template. (c) TEM images of F127 NR-1 showing a typical uniform organization that contains between two and eight nanoparticles. Most of the products are dimers, trimers, and tetramers of nanoparticles. The spacing between nanoparticles is clearly discernible (>1 nm).

the medium-length products (~60-nm) are dominant. The diameter of P123 NR varies from 5 to 7.0 nm, with a standard derivation ~10%, i.e., $L/D = 10.0 \pm 13\%$ for $L = 60$ nm and $L/D = 7.0 \pm 13\%$ for $L = 90$ nm. The average L/D ratio of the products is larger than that of CdSe nanorods synthesized from a two-surfactant system (for which $L/D = 1.1-5.0$, with L between 5.1 ± 0.8 and 21.8 ± 4.2 nm),[9] and the diameter distribution is much narrower than that of the CdS nanorods synthesized from ionic cetyltrimethylammonium bromide (CTAB) copolymer (for which $L/D \approx 6.5$, with diameters varying from 7 to 14 nm).[24]

(2) F127 $[(EO)_{106}(PO)_{70}(EO)_{106}]$, $f = 3.03$. The polyethylene unit of F127, $(EO)_x$ with $x = 106$, is much longer than that of P123. Figure 3c shows that the morphology of the product, synthesized using the same mole ratio as used in the synthesis of P123 NR-1, is a uniform organization of between two and eight nanoparticles (F127 NR-1). Most of the products consist of dimers, trimers, and tetramers of nanoparticles. The space between the nanoparticles is clearly discernible (>1 nm). The diameter of the F127 NR-1 nanoparticles varies from 4.5 to 7.0 nm, which is close to the diameter of P123 NR-1.

(3) L64 $[(EO)_{13}(PO)_{70}(EO)_{13}]$, $f = 0.37$, and L121 $[(EO)_5(PO)_{70}(EO)_5]$, $f = 0.14$. L64 has a much smaller $(EO)_x$ fraction, $x = 13$, than do P123 ($x = 20$) and F127 ($x = 106$). The morphology of the major product synthesized from the L64 copolymer is a lamellar (smetic) multilayer material, L64 NR-1. Select area electron diffraction (SAED) pattern and XRD results show that L64 NR-1 is amorphous. The structural transition from P123 NR-1 to L64 NR-1 is probably due to the change in the (EO)/(PO) ratio,[25] but it might also be affected by the overall length of the polymer (N). The L121 copolymer has the shortest $(EO)_x$ fraction in the $(EO)_x$-$(PO)_{70}(EO)_x$ series, $x = 5$. In the TEM image of the L121 final product, no nanorods, nanoparticles, or multilayer material can be found, and a large amount of chunky material is observed.

(b) Effect of the $(PO)_y$ Fraction on the Morphology and Diameter of CdS Nanocrystals. (1) P65 $[(EO)_{20}(PO)_{30}$-

(24) Chen, C.-C.; Chao, C.-Y.; Lang, Z.-H. *Chem. Mater.* **2000**, *12*, 1516−1518.

(25) Diat, O.; Roux, D. J. *J. Phy. II* **1993**, *3*, 9.

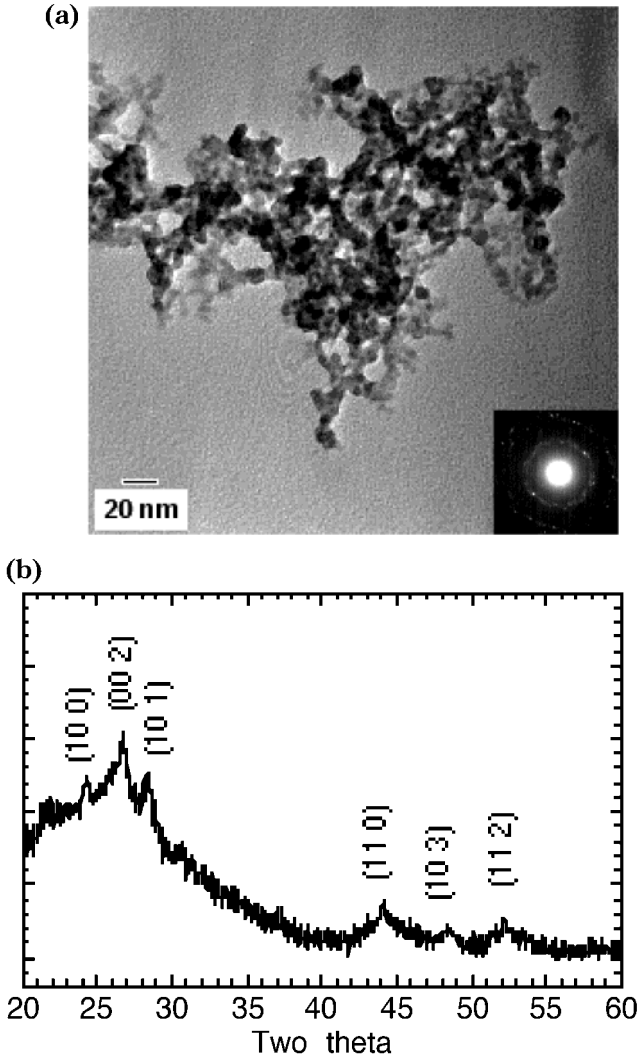

Figure 4. (a) Net-like array morphology of P65 NR-1. The diameters of P65 NR-1 crystals vary from 4.5 to 6.5 nm, which is slightly smaller than the diameters of P123 NR-1. Select area electron diffraction (SAED) confirms the polycrystalline structure of P65 NR-1. (b) XRD pattern for P65 NR-1. It is consistent with the hexagonal wurtzite crystal phase.

$(EO)_{20}$], $f = 1.33$, and F68 [$(EO)_{80}(PO)_{30}(EO)_{80}$], $f = 5.33$. After the effect of the $(EO)_x$ fraction on the morphology and diameter of product had been examined, P65 and F68 were chosen for an investigation of the effect of changing the $(PO)_y$ fraction on the evolution of the morphology of the product. P65 has the same $(EO)_x$ length as P123 but fewer $(PO)_y$ units. F68 has an $(EO)_x$ length close to that of F127 but a much shorter $(PO)_y$ segment. The f value for F68 is significant higher than the f values for the other polymers studied in this paper.

Figure 4a shows the TEM image of the product synthesized using P65 by the same route as P123 NR-1. The morphology of the product is a net-like array of linked nanoparticles (P65 NR-1) and is obviously different from the structures obtained with P123 NR-1 and F127 NR-1. Select area electron diffraction (SAED), inset in Figure 4a, confirms the polycrystalline structure of P123 NR-1. A similar CdS nanocrystal network structure by a solution route has been obtained with an average diameter of 7.0 nm using polyphosphazene polymer matrix as the template.[23] The diameter of P65 NR-1 varies from 4.5 to 6.5 nm, which is slightly smaller than the diameter obtained with polyphosphazene and P123 NR-1 (5.0−7.0 nm). The XRD pattern (Figure 4b) of P65 NR-1 is consistent with the hexagonal wurtzite structure. In the F68 case, the structure of the final product is a disordered material that contains a large number of aggregated very small nanoparticles with diameters < 2.5 nm. No evidence for nanorods or aligned nanoparticles could be found in the TEM images. The SAED and XRD patterns show that these aggregated nanoparticles are amorphous.

(3) Effect of Concentration and Temperature on the Evolution of the Morphology of the CdS Nanocrystals. Two surfactants were chosen for a study of the effects of the mole ratio and the temperature on the evolution of the morphology of the CdS nanocrystals: P123 and F127. The mole ratio between the surfactant and water is kept constant, and only the concentrations of precursors are varied.

(a) Concentration Effect. (1) P123/Cd^{2+}/S^{2-}/H_2O = 1:16:16:10 000. If the concentrations of Cd^{2+} and S^{2-} are increased to 60% higher than those used for P123 NR-1, the morphology of the new product (P123 NR-2) does not show any apparent change from that of P123 NR-1. That is because the mole ratio between surfactant and water is kept constant. The diameter distribution of P123 NR-2 still maintains the convergence $L/D = 8.0 \pm 20\%$, with diameters from 5.0 to 9.0 nm and lengths from 30 to 90 nm. Figure 5a shows the high-resolution TEM image of P123 NR-2, obtained using a JEOL 2010HR instrument, formed by a linkage of nanoparticles in a single-column chain. The appearance of a large number of nanoparticles in this micrograph is another interesting result, which suggests that the morphology of the product could be controlled by varying the concentrations of the starting reagents. The unusual nanoparticle-linkage structure for P123 NR-2 has not been previously reported. There is no TEM evidence to show obvious fusion or overlapping between nanoparticles that compose P123 NR-2. P123 NR-2 was annealed in glyme at 65 °C for 60 min for X-ray diffraction (XRD) measurements. The XRD pattern of P123 NR-2 agrees with the hexagonal wurtzite structure, shown in Figure 5b, and is consistent with the diameter data obtained from the TEM image ($R \approx 8.0$ nm).

(2) F127/Cd^{2+}/S^{2-}/H_2O = 1:16:16:10 000. To make a comparison with the P123 case, the concentrations of Cd^{2+} and S^{2-} in this reaction were increased to 60% higher than those used for F127 NR-1. Figure 5c shows the TEM image of the product, F127 NR-2. The diameter distribution of F127 NR-2 ranges from 4.5 to 10.0 nm. The phenomenon of nanoparticle alignment still exists. F127 NR-2 has a tendency to nucleate and array the semiconductor nanoparticles in three dimensions with roughly similar spacings between them. The high-resolution TEM micrograph (Figure 5d) for one of the F127 NR-2 nanocrystallites in the correct orientation to show the d spacings of the lattices fringes (3.35 Å) is consistent with the {002} crystal plane of wurtzite-structured CdS. The F127 NR-2 XRD sample was prepared by annealing at 65 °C for 60 min, the same preparation as for the P123 NR-2 XRD sample. The diffraction pattern (Figure 5e) matches the hexagonal wurtzite symmetry and there is no evidence of a mixed phase. Figure 5f shows the room-temperature UV−

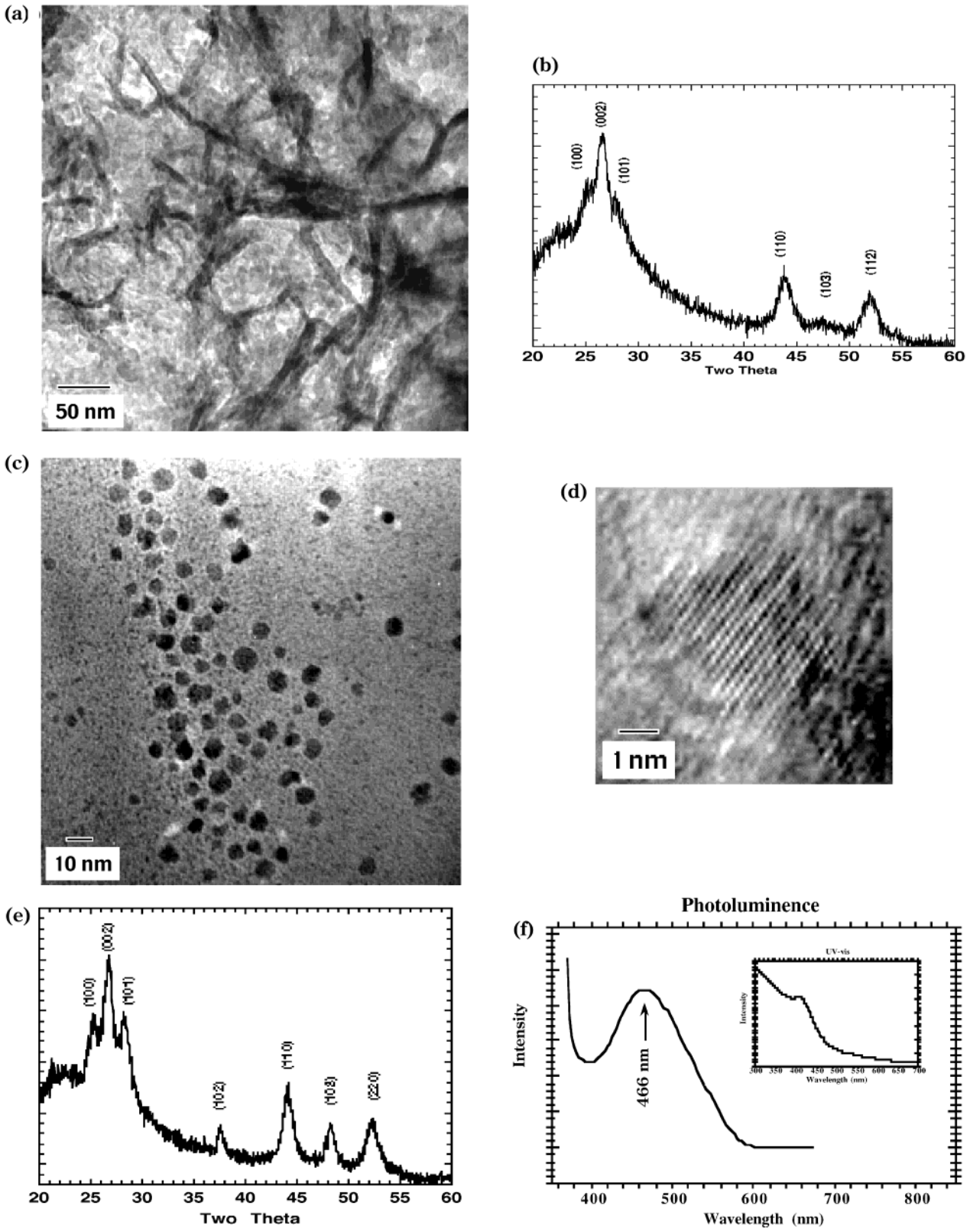

Figure 5. (a) High-resolution TEM image for P123 NR-2. It shows that the CdS NR-1 structure is formed by a linkage of nanoparticles as a single-column chain. The average diameter of P123 NR-2 is similar to that of P123 NR-1. (b) X-ray powder diffraction pattern of P123 NR-2, which is consistent with the hexagonal wurtzite symmetry. (c) Micrograph showing a large number of nanoparticles synthesized with the F127 triblock copolymers system. The phenomenon of nanoparticle alignment still exists. F127 NR-2 has the tendency to nucleate and array the semiconductor nanoparticles in three dimensions. (d) High-resolution TEM micrograph for one of the F127 NR-2 nanocrystallites. The *d* spacing of the lattices fringes (3.35 Å) is consistent with the {002} crystal plane of wurtzite-structured CdS. (e) X-ray powder diffraction pattern of F123 NR-2, which is consistent with the hexagonal wurtzite symmetry and shows no envidence of a mixed phase. (f) Room-temperature UV−visible absorption spectrum (inset) and photoluminescence (PL) spectrum. The λ_{max} of the PL peak is at about 466 nm and the half-width is smaller than 70 nm, which is close to that of UV−vis peak (∼40 nm).

visible absorption spectrum (inset) and the photoluminescence (PL) spectrum. The λ_{max} of the PL peak is at about 466 nm, with a half-width smaller than 70 nm, which is close to that of UV−vis peak (~40 nm). The long-tail peak associated with deep trap states due to surface or core defects is not evident in this sample.

(b) Temperature Effect. It is generally believed that temperature plays an important role in determining the morphology and quality of nanocrystals. The reactions followed exactly the same route as that used for P123 NR-1 and F127 NR-1 except the reaction temperature was changed to 25 and 65 °C.

(1) Synthesis of P123 NR at 25 and 65 °C. Two reactions were carried out simultaneously to synthesize P123 NR. The temperature of one reaction was held at 25 °C (P123 NR-3) and the other at 65 °C (P123 NR-4). TEM images of P123 NR-3 show that the diameter distribution of the product is from 4.5 to 6.0 nm ($\sigma \approx$ 8%) with lengths of 25−75 nm. The distribution of diameters of P123 NR-3 is roughly similar to that of P123 NR-1, but the lengths are about 50% smaller. The XRD pattern of P123 NR-3 shows that the product is not crystalline unless it is annealed in glyme at 65 °C for 1 h. The TEM images of P123 NR-4 indicate that the crystals 5.5−8.0 nm in diameter ($\sigma \approx$ 10%) and 25−125 nm in length, as shown in Figure 6a. The XRD pattern of P123 NR-4 was measured directly from the product obtained by precipitation from solution without any further annealing. The diffraction pattern agrees with the expected hexagonal wurtzite crystal plane (Figure 6b). These results confirm that the crystal quality of CdS nanocrystals is highly dependent on the reaction temperature.

(2) Synthesis of F127 NR at 25 and 65 °C. The same reaction conditions were used for the synthesis of F127 NR-3 (25 °C) and F127 NR-4 (65 °C). An obvious aggregation of nanoparticles was shown in the F127 NR-4 TEM image of the final product. The space between nanoparticles is filled, and the morphology is roughly similar to that of P65 NR-1. The diameter of F127 NR-4 varied from 8.5 to 11.5 nm, which is larger than the diameters of P65 NR-1 and F127 NR-1. In the F127 NR-3 reaction, no nanoparticles or nanorods could be found in the TEM images of the product. The morphology of the final product shown in the TEM micrograph is an agglomeration of a large amount of feather-shaped amorphous material.

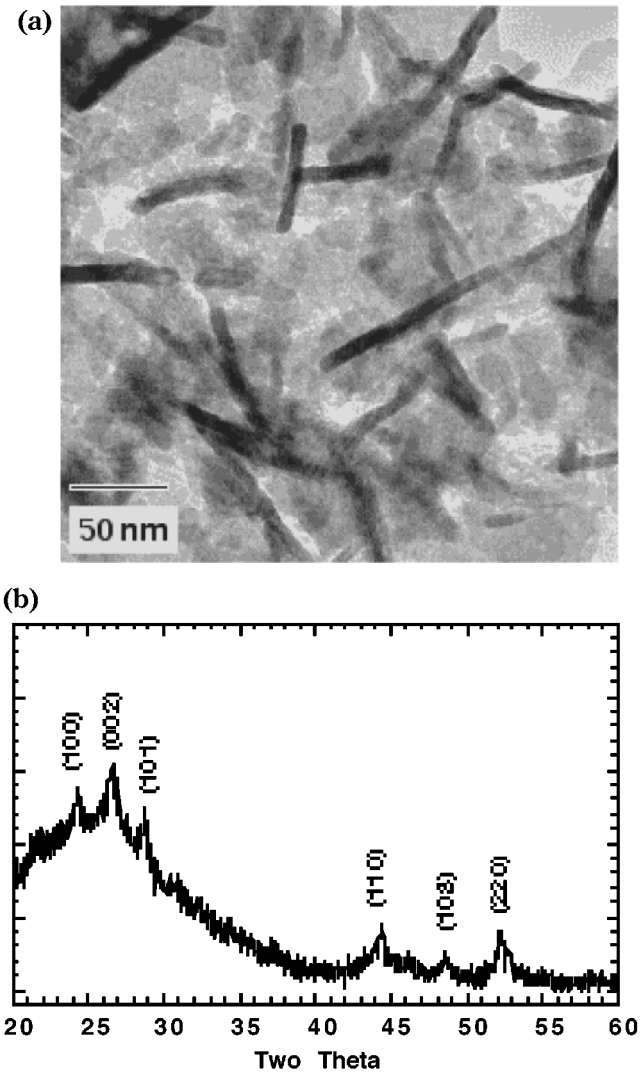

Figure 6. (a) TEM image of P123 NR-4 showing that P123 NR-4 is 5.5−8.0 nm in diameter and 25−125 nm in length. (b) Typical X-ray diffraction pattern for P123 NR-4. The diameter value derived from the (110) peak using the Scherrer equation is about 9.0 nm, which is consistent with the data obtained from the TEM images.

Discussion

(I) CdS Microrods and Microparticles. Table 1 lists the reaction conditions and the size data for products synthesized in EG, glyme, and EG/glyme mixed solvent without surfactant. The results show that an increase in the amount of glyme leads to a decrease in the size of the rods and that the morphology of the rods is highly effected by the volume ratio of EG and glyme in the mixed solvent. In the 100% EG reaction, microrods are the only morphology shown in the final product. On the other hand, in the 100% glyme reaction, spherical microparticles with porous surfaces dominate the final product, with small amounts of rod-1 and rod-2 products. The dumbbell-shaped products appeared mainly in the reaction in which EG is the major component of the solvent. In our SEM micrographs of the products, sharp-ended microrods are unlikely to be found.

(II) CdS Nanorods and Nanoparticles. Table 2 lists the reaction conditions and sizes of the CdS nanorods and nanoparticles synthesized using $(EO)_x$-$(PO)_y(EO)_x$ triblock copolymers at low temperature (25−65 °C). The self-assembly mechanism of triblock copolymers in the aqueous phase has been well-known for years.[12,26,27] The equilibrium of the triblock copolymer system will change upon addition of inorganic precursors, and a new competition among all species, including unimers, will be triggered until a new equilibrium is reached.[28] The precise metal cations coordinated and the extended nanoarray templating conditions for the crystal growth of CdS nanocrystals in triblock copolymers

(26) Pileni, M. P. *Langmuir* **1997**, *13*, 3266−3276.
(27) Alexandridis, P.; Olsson, U.; Lindman, B. *Langmuir* **1998**, *14*, 4, 2627−2638.
(28) Nagarajan, R. *Colloids Surf. B: Biointerfaces* **1999**, *16*, 55−72.

Table 1. Reaction Conditions and Results of High-Temperature Synthesis without Surfactant

solvent	product color	morphology	size data[a]
100% EG	yellow	uniform flat-ended rods	$L > 4\ \mu$m, $R = 0.2-0.6\ \mu$m
80% EG + 20% glyme	yellow	dumbbell-shaped rods	$L \approx 2\ \mu$m, $R = 0.25-0.35\ \mu$m
50% EG + 50% glyme	yellow	dumbbell-shaped rods	$L \approx 1\ \mu$m, $R = 0.3-0.4\ \mu$m
100% glyme	yellow	giant spherical particles	$R \approx 0.55-0.75\ \mu$m

[a] L = length, R = diameter, reaction time= 4 h.

Table 2. Reaction Conditions and Size Data for Low-Temperature Synthesis with Surfactant

triblock copolymer $(EO)_x(PO)_y(EO)_x$	f $(2x/y)$	product color	morphology	size data[a]
Pluronic L121 $(EO)_5(PO)_{70}(EO)_5$	0.14	yellow-green	chunky material	
Pluronic P123 $(EO)_{20}(PO)_{70}(EO)_{20}$	0.57	orange	nanorods	(NR-1) $L = 30-90$ nm, $R = 5.0-7.0$ nm (NR-2) $L = 30-90$ nm, $R = 5.0-9.0$ nm (NR-3) $L = 25-75$ nm, $R = 4.5-6.0$ nm (NR-4) $L = 25-125$ nm, $R = 5.5-8.0$ nm
Pluronic L64 $(EO)_{13}(PO)_{30}(EO)_{13}$	0.87	yellow	multilayer phase	
Pluronic F127 $(EO)_{106}(PO)_{70}(EO)_{106}$	3.03	tangerine	aligned nanoparticles	(NR-1) $R = 4.5-7.0$ nm (NR-2) $R = 4.5-10.0$.nm (NR-4) $R = 8.5-11.5$ nm
Pluronic P65 $(EO)_{20}(PO)_{30}(EO)_{20}$	1.33	orange	network nanorods	$R = 4.5-6.5$ nm
Pluronic F68 $(EO)_{80}(PO)_{30}(EO)_{80}$	5.33	orange	aggregated small nanoparticles	$R < 2.5$ nm

[a] L = length, R = diameter, reaction time= 16 h.

system have not been solved but it is clear that both the hydrophilic $(EO)_x$ and the hydrophobic $(PO)_y$ fractions will affect the growth of the CdS seeds.[28−30] The diameters of the nanoparticle are affected by the length of the $(PO)_y$ fraction of surfactant. For example, the diameter of P123 NR-2 [$(PO)_y$ with $y = 70$] (5.0−9.0 nm) is larger than the diameter of P65 NR-1 [$(PO)_y$ with $y = 30$] (4.5−6.5 nnm). In addition to the growth of the nanoparticles, the f value of the triblock copolymers strongly affects the linking mechanism between the nanoparticles. In the P123 NR-2 case ($f = 1.33$), there is no discernible evidence from TEM of spacings between the linking nanoparticles. However, in F127 NR-1 ($f = 3.03$), the spacing between aligned nanoparticles is clearly shown in the TEM micrographs. In the concentration effect study, the TEM images of P123 NR-2 and P123 NR-1 show that the morphologies of the nanorods can be controlled by varying the mole ratio between the triblock copolymers and the inorganic precursors. Although there is doubt that the linking mechanism of the NRs depends strongly on the coordinating force of the surfactant, the precise mechanism for the formation of CdS NRs from CdS nanoparticles requires additional experimental data. However, the linkage mechanism for nanoparticles templated by triblock copolymer P123 is known to be highly dependent on the concentration and the amphiphilic properties of the surfactant itself, as well as the polarity of solvent.[12,27] It will be very helpful to further investigate the effect of changing the volume ratio of the hydrophilic and hydrophobic fractions, for example by changing the hydrophobic part from propylene oxide to butylene oxide.

Summary

In this paper, we show the potential of $(EO)_x(PO)_y(EO)_x$ triblock copolymers to be used as surfactant templates in the synthesis of CdS nanorods and nanoparticles at low temperature (25−65 °C) via the reaction of cadmium acetate and sodium sulfide in an organic solvent without surfactant and in an aqueous phase with surfactant. In the organic solvent without surfactant route, the stronger chelating active sites and the weaker intermolecular coordination of the solvent help the growth of the rods to reach several micrometers in length and about 0.4 μm in width. The use of Pluronic triblock copolymers as surfactant templates in aqueous solution shows considerable potential for the synthesis of CdS NRs and nanoparticles. The (EO)/(PO) hydrophilic/hydrophobic ratio, f, is an important factor in determining the morphology of the final products. For example, in the P123 NR-1 case, f offers the opportunity to grow NRs with a narrow diameter distribution that varies from 5 to 7.0 nm and with lengths from 30 to 90 nm.

Acknowledgment. This research was supported by the National Science Foundation (Grants DMR 96-34396 and DMR 98-71849) and the Office of Naval Research (Grant ONR N00014-99-1-0728). Work at the Materials Research Laboratory (MRL), UC Santa Barbara, made use of MRL Central Facilities supported by the National Science Foundation under Award DMR 96-32716.

CM011227B

(29) Braun, P. V.; Stupp, S. I. *Mater. Res. Bull.* **1999**, *34*, 463−469.

(30) Braun, P. V.; Osenar, P.; Tohver, V.; Kennedy, S. B.; Stupp, S. I. *J. Am. Chem. Soc.* **1999**, *121*, 7302−7309.